10-27-2015

Cyclic Di-GMP-Mediated Repression of Swarming Motility by Pseudomonas aeruginosa PA14 Requires the MotAB Stator

S. L. Kuchma
Dartmouth College

N. J. Delalez
University of Oxford

L. M. Filkins
Dartmouth College

E. A. Snavely
Dartmouth College

J. P. Armitage
University of Oxford

See next page for additional authors

JB Journals.ASM.org

Cyclic Di-GMP-Mediated Repression of Swarming Motility by *Pseudomonas aeruginosa* PA14 Requires the MotAB Stator

S. L. Kuchma,[a] N. J. Delalez,[b] L. M. Filkins,[a] E. A. Snavely,[a]* J. P. Armitage,[b] G. A. O'Toole[a]

Department of Microbiology and Immunology, Geisel School of Medicine at Dartmouth, Hanover, New Hampshire, USA[a]; Department of Biochemistry, University of Oxford, Oxford, United Kingdom[b]

The second messenger cyclic diguanylate (c-di-GMP) plays a critical role in the regulation of motility. In *Pseudomonas aeruginosa* PA14, c-di-GMP inversely controls biofilm formation and surface swarming motility, with high levels of this dinucleotide signal stimulating biofilm formation and repressing swarming. *P. aeruginosa* encodes two stator complexes, MotAB and MotCD, that participate in the function of its single polar flagellum. Here we show that the repression of swarming motility requires a functional MotAB stator complex. Mutating the *motAB* genes restores swarming motility to a strain with artificially elevated levels of c-di-GMP as well as stimulates swarming in the wild-type strain, while overexpression of MotA from a plasmid represses swarming motility. Using point mutations in MotA and the FliG rotor protein of the motor supports the conclusion that MotA-FliG interactions are critical for c-di-GMP-mediated swarming inhibition. Finally, we show that high c-di-GMP levels affect the localization of a green fluorescent protein (GFP)-MotD fusion, indicating a mechanism whereby this second messenger has an impact on MotCD function. We propose that when c-di-GMP level is high, the MotAB stator can displace MotCD from the motor, thereby affecting motor function. Our data suggest a newly identified means of c-di-GMP-mediated control of surface motility, perhaps conserved among *Pseudomonas*, *Xanthomonas*, and other organisms that encode two stator systems.

Since its discovery in 1987 as an allosteric activator of bacterial cellulose synthesis (1), cyclic diguanylate (c-di-GMP) has been shown to be a remarkably important signaling molecule across diverse bacterial species, controlling a multitude of behaviors and processes, including biofilm formation, motility, virulence, cell cycle progression, and differentiation (2–4). An important feature of c-di-GMP regulation is the ability of this signal to control critical lifestyle transitions, such as motile-sessile transitions (e.g., planktonic to biofilm), which are undertaken by many bacterial species (3, 5, 6). Generally speaking, elevated levels of c-di-GMP promote sessile lifestyles such as biofilm formation; in contrast, low levels of c-di-GMP are associated with motility (3, 6). Intracellular levels of this dinucleotide are controlled by opposing activities of enzymes that synthesize c-di-GMP (GGDEF domain-containing diguanylate cyclases [DGCs]) and those that cleave this signaling molecule (EAL- or HD-GYP domain-containing phosphodiesterases [PDEs]) (3, 4, 7–11).

More recently, studies focused on how cells respond to changing c-di-GMP levels, indicated that this signaling network relies upon proteins or RNA molecules, known as c-di-GMP effectors (or receptors), which bind c-di-GMP and whose output functions are altered due to c-di-GMP-mediated structural changes (3, 4, 12). A number of distinct effectors have been identified and classified based on their c-di-GMP-binding motif. The PilZ class of c-di-GMP effector proteins is one of the best-studied classes to date, with homologs across multiple bacterial species (2, 13, 14). PilZ domain proteins, such as YcgR, play a critical role in the c-di-GMP-dependent control of swimming motility in *Escherichia coli* and *Salmonella enterica* (14–18), and the recently identified FlgZ participates in the regulation of swimming motility by *Pseudomonas fluorescens* F113 and *Pseudomonas putida* KT2440 (19). While the precise mechanism of PilZ-dependent control of motility is still controversial, the models presented to date suggest that the PilZ–c-di-GMP complex impacts flagellar motor function (2, 15, 16, 18, 20). Motility can also be impacted by production of exopolysaccharides or through transcriptional control of the flagellar biosynthesis machinery (21–24).

Here we have uncovered a new c-di-GMP-dependent mechanism of motility control in *P. aeruginosa*, a microbe with two stator sets and a single rotor available to mediate function of its single polar flagellum. This dinucleotide controls an apparent "stator swapping" mechanism. MotCD is the stator responsible for driving swarming motility in *P. aeruginosa*, while the MotAB stator is unable to support swarming. Under conditions of high c-di-GMP, the MotAB stators are involved in the repression of swarming. Deleting *motAB* or introducing point mutations into *motA* that are predicted to disrupt key interactions with FliG, the rotor component of the motor, relieves this c-di-GMP-mediated repression of swarming. Furthermore, under conditions of high c-di-GMP, we observed altered localization of a GFP-MotD fusion. Taking these data together, we propose a model wherein, under conditions of high c-di-GMP levels, MotAB participates in repression of swarming motility, perhaps by replacing or displacing the MotCD stators in the flagellar motor.

Received 23 July 2014 **Accepted** 20 October 2014

Accepted manuscript posted online 27 October 2014

Citation Kuchma SL, Delalez NJ, Filkins LM, Snavely EA, Armitage JP, O'Toole GA. 2015. Cyclic di-GMP-mediated repression of swarming motility by *Pseudomonas aeruginosa* PA14 requires the MotAB stator. J Bacteriol 197:420–430. doi:10.1128/JB.02130-14.

Editor: T. J. Silhavy

Address correspondence to G. A. O'Toole, georgeo@dartmouth.edu.

* Present address: E. A. Snavely, Department of Molecular Genetics and Microbiology, Duke University, Durham, North Carolina, USA.

Supplemental material for this article may be found at http://dx.doi.org/10.1128/JB.02130-14.

doi:10.1128/JB.02130-14

MATERIALS AND METHODS

Strains and media. Strains used in this study are listed in Table S1 in the supplemental material. *P. aeruginosa* PA14, *E. coli* DH5α, S17-1 λpir, BTH101, JM109, and XL-Blue were routinely cultured in lysogeny broth (LB) medium, solidified with 1.5% agar when necessary. Gentamicin (Gm) was used at 25 μg/ml for *P. aeruginosa* and at 10 μg/ml for *E. coli*. Ampicillin (Ap) was used at 150 μg/ml, nalidixic acid (NA) at 20 μg/ml, streptomycin at 100 μg/ml, kanamycin at 50 μg/ml, and carbenicillin at 100 μg/ml for *E. coli*. For phenotypic assays with *P. aeruginosa*, either M63 or M8 minimal salts medium (as indicated) were supplemented with $MgSO_4$ (1 mM), glucose (0.2%), and Casamino Acids (CAA; 0.5%). For expression plasmids harboring the P_{BAD} promoter, arabinose was added to cultures at a 0.2% final concentration, unless noted otherwise. For plating of bacterial two-hybrid assays, X-Gal (5-bromo-4-chloro-3-indolyl-β-D-galactopyranoside; 40 μg/ml) and IPTG (0.5 mM) were added to selective plates to visualize β-galactosidase reporter expression.

Saccharomyces cerevisiae strain InvSc1 (Invitrogen), used for plasmid construction via *in vivo* homologous recombination, was grown with yeast extract-peptone-dextrose (1% Bacto yeast extract, 2% Bacto peptone, and 2% dextrose), as reported previously (25). Selections with InvSc1 were performed using synthetic defined agar-uracil (4813-065; Qbiogene).

Construction of mutant strains and plasmids. Table S2 in the supplemental material lists all plasmids used in this study. Primers used in plasmid construction and in mutant construction and confirmation are listed in Table S3 in the supplemental material. In-frame gene deletions, chromosomal "knock-in" procedures for epitope tagging, mutagenesis, and complementation were performed via allelic exchange, as reported previously (26, 27). Plasmids for these purposes were constructed via cloning by homologous recombination of relevant PCR products into the pMQ30 vector in yeast, as reported (25).

Motility assays. Swim (0.3% agar) and swarm (0.5% agar) motility plates contained M8 medium supplemented with glucose, $MgSO_4$, CAA, and arabinose, where indicated. Swim assays were performed as previously described (28). Swarm assays were performed as previously described (29). Quantification of swim and swarm zones was performed using ImageJ software.

Biofilm formation assay. Biofilm formation in 96-well microtiter plates was assayed and quantified as previously described (30, 31). All biofilm assays were performed using M63 minimal medium supplemented with glucose, $MgSO_4$, CAA, and arabinose where indicated.

CR binding assays. Congo red (CR) binding assays were performed as reported previously (32–34).

Protein expression and cellular localization experiments. Strains were cultured on semisolid agar (0.5%) swarm plates and cells were allowed to swarm for 16 h at 37°C, followed by harvesting by gentle scraping with an ethanol-washed plastic coverslip into microcentrifuge tubes and samples were centrifuged for 1 min at room temperature (RT). Supernatants were removed, and cell pellets were frozen at −80°C until further processing was performed. For generation of whole-cell (WC) lysates, cell pellets were then resuspended in cell lysis buffer (200 mM Tris-HCl [pH 7.5], 1 mM EDTA, 2 mM $MgCl_2$, complete protease inhibitors [Roche Diagnostics Corp., Indianapolis, IN]), and Benzonase nuclease (Novagen, San Diego, CA) was added to a final concentration of ~50 units/ml. Bacterial cells were lysed in a French pressure cell, and samples were centrifuged at 9,300 × *g* for 10 min at 4°C to remove unbroken cells. Supernatants were collected as whole-cell lysates, and, where indicated, samples were further fractionated to yield cytoplasmic, inner membrane, and outer membrane fractions, as described previously (34–36).

For Western blotting, WC lysates and fractions were prepared as described previously (37) with the exception that samples were resolved by SDS-PAGE using 12% polyacrylamide gels. Proteins transferred to a nitrocellulose membrane were probed with either an anti-penta-His antibody (Qiagen, Valencia, CA) or an antihemagglutinin (anti-HA) antibody (Covance, Princeton, NJ). Detection of proteins and quantification of protein levels were performed as previously described (37).

Bacterial two-hybrid analysis. The bacterial adenylate cyclase two-hybrid (BACTH) system developed by Euromedex (Souffelweyersheim, France), based on published work (38), was used in this study. Experiments were performed according to the manufacturer's instructions.

Fluorescence microscopy. Cells were grown on 0.5% agar swarm plates at 37°C for 14 to 18 h, as described previously (34). Cells were picked from the edges of the swarm branches just before imaging and embedded in 1.2% agarose on a microscope slide. A home-built inverted microscope with a 473-nm laser (50 mW, 473-50-COL-002; Laser 2000) was used, as described previously (39). Laser epifluorescence illumination was used for all fluorescence imaging of the motor spots with laser intensity of ~0.1 $\mu W \cdot \mu m^{-2}$. Fluorescence emissions of the GFP-labeled motor spots were imaged in frame transfer mode at 50 nm/pixel and 25 Hz using a 128- by 128-pixel, cooled, back-thinned electron-multiplying charge-coupled device camera (iXon DV860-BI; Andor Technology). For each field of view, 300 frames were recorded, and the number of cells with a polar spot was determined manually using ImageJ.

RESULTS

MotAB flagellar stator proteins participate in c-di-GMP-mediated swarming inhibition. Previously, we reported the use of a genetic screen to identify factors required to repress swarming motility via the intracellular second messenger cyclic diguanylate (c-di-GMP) (34). For this screen, we exploited the swarming defect of a mutant strain bearing a deletion of the *bifA* gene (PA4367), which encodes a c-di-GMP-degrading PDE. We have shown that loss of the BifA PDE leads to an accumulation of intracellular c-di-GMP levels relative to the wild-type strain, resulting in failure of the Δ*bifA* mutant to swarm (34, 35) (Fig. 1A, top). We performed mutagenesis of the Δ*bifA* mutant using the *mariner* transposon and screened for restoration of swarming motility.

In our previous study, we screened approximately 5,500 transposon mutants for suppressor strains that regained the ability to swarm on semisolid agar (34). Given that our genetic screen had not achieved a full coverage of the *Pseudomonas* genome (~6,000 genes), we continued with *mariner* mutagenesis of the Δ*bifA* mutant and screened an additional ~10,500 transposon insertion mutants. From this screen, we isolated 23 mutant strains that regained the ability to swarm, and we mapped the transposon insertions in these mutants to 12 different genes (see the supplemental material for a complete list of suppressor strains, gene designations, and phenotypic summaries). This screen identified mutations in genes or operons that we, or others, have characterized previously (*sadB*, *pilY1*, *pel*, and *gacS*) (30, 32, 34, 35, 40–42), mutations that likely exerted their effects through polarity on downstream functions (*pvrS*, *fimU*, and *cupA*), and a mutation in one gene that encodes a predicted DGC-PDE dual domain protein (43). A more detailed description of the mutants identified is included in the supplemental material and in Table S4 in the supplemental material.

There were three additional strains that fully recovered the ability to swarm, and each strain harbored an insertion that mapped to the *motA* gene (PA14_65450) (see Table S4 in the supplemental material). Strains with mutations in the *motA* gene were not isolated in the previous screen (34), confirming that the earlier screen had not reached saturation. The swarm phenotype of a representative suppressor strain (Δ*bifA motA*::Mar) is shown in Fig. 1A (top panel, third column from the left). As shown, this double mutant regained the ability to form tendril-like projections from the point of inoculation, in contrast to the Δ*bifA* mu-

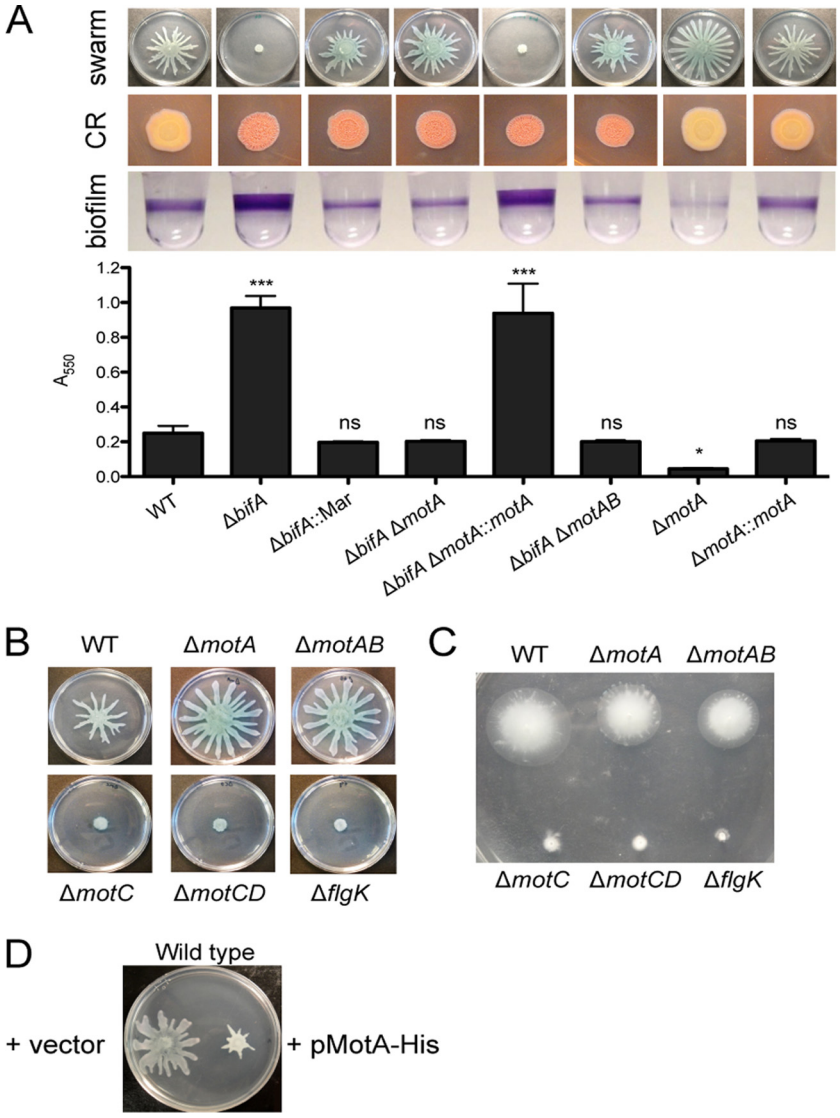

FIG 1 Phenotypic analyses of flagellar stator mutant strains. (A) Assessment of *motA* and *motAB* mutation on suppression of Δ*bifA* mutant phenotypes. The strain genotype for each image in this panel is located along the *x* axis of the graph. The top row shows representative swarm images for the wild type and the Δ*bifA* mutant, followed by a representative Δ*bifA motA*::Mar suppressor strain (66B5), the Δ*bifA* Δ*motA* double mutant, the Δ*bifA* Δ*motA*::*motA* complemented strain, the Δ*bifA* Δ*motAB* triple mutant, the single Δ*motA* deletion mutant, and its complemented counterpart strain Δ*motA*::*motA*. Swarm plates were incubated at 37°C for 16 h. The second row shows CR binding for each strain. CR assay plates were incubated at 37°C for 24 h, followed by 48 h at room temperature. The bottom row shows images of wells from a 96-well biofilm assay plate. Strains were grown in M63 medium supplemented with glucose, $MgSO_4$, and CAA for 24 h prior to crystal violet (CV) staining. The graph depicts quantification of CV-stained biofilms. CV was solubilized in 30% glacial acetic acid, and the absorbance was read at 550 nm. Error bars indicate standard deviations of the average of three experiments with four replicates per experiment. Data were analyzed by one-way analysis of variance (ANOVA) followed by Tukey's posttest comparison. ns, not significantly different; *, $P < 0.05$; ***, $P < 0.001$ (all relative to the wild type). (B and C) Representative swarm (B) and 0.3% soft-agar (C) motility assays of the strains indicated. The Δ*flgK* mutant does not make a flagellum and serves as a negative control in both assays. Swarm and soft-agar motility plates were incubated at 37°C for 16 h. (D) Impact of *motA* overexpression on swarming motility. The image is of a representative plate showing repression of swarming motility by overexpression of the multicopy pMotA-His plasmid (right) relative to the vector control (left). Arabinose was added to a final concentration of 0.2%, and plates were incubated at 37°C for 16 h.

tant alone, and demonstrated swarming comparable to that of the wild type (Fig. 1A, top panel, leftmost image).

The *motA* gene encodes a component of the flagellar stator complex that, with MotB, forms the peptidoglycan-bound proton translocating complex that functions to power rotation of the flagellar rotor (44–46). Thus, we next asked whether suppression by the *motA* mutation is specific to the swarming motility defects of the Δ*bifA* mutant or whether additional c-di-GMP-related phenotypes are also affected. We therefore tested whether mutations in *motA* might also impact swimming, Pel polysaccharide production, and/or biofilm formation.

In the "swim" assay, cells move within the liquid of the 0.3% soft agar of the plate, as opposed to swarming motility, which occurs on the surface of the semisolid agar plate (28, 29). This soft-agar-based swim assay reflects the functionality of the flagellum, as well as the chemotaxis machinery. Thus, in these experiments, we used this low-percentage-agar assay as a surrogate to judge the functionality of the flagellar machinery. The Δ*bifA* mu-

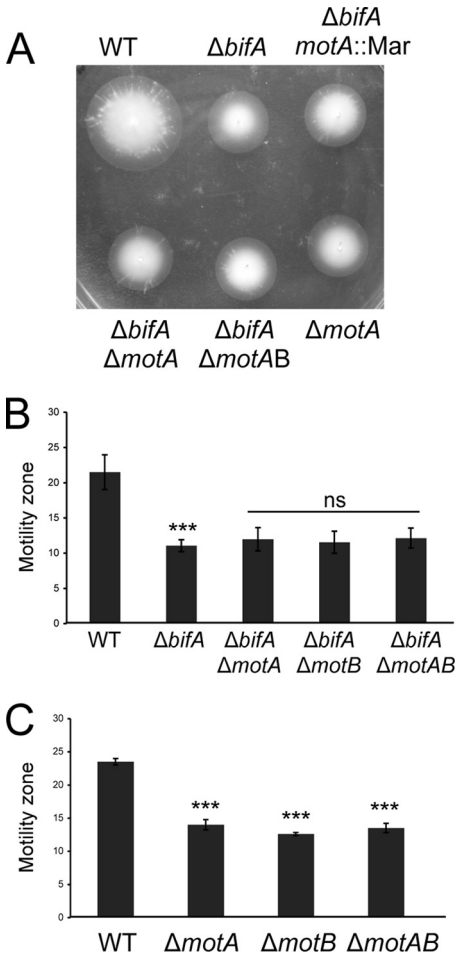

FIG 2 Soft-agar motility assays of Δ*bifA* and stator mutants. (A) Representative motility assay of the indicated strains. Soft-agar plates (0.3% agar) were incubated at 37°C for 16 h. (B and C) Motility zone measurements are shown for the 0.3% soft-agar assay with the indicated strains. Measurements were obtained using Image J, with units in pixels ($\times 10^4$). Error bars indicate standard deviations of the averages from three experiments with six replicate plates per experiment. Data were analyzed by one-way analysis of variance followed by a Tukey's posttest comparison. ns, not significantly different; ***, $P < 0.001$. In panel B, the Δ*bifA* mutant is compared to the wild type and the Δ*bifA mot* mutants are compared to the Δ*bifA* mutant, and in panel C, statistical comparisons are relative to the wild type.

tant exhibits reduced motility (~50% of wild type) in soft-agar plates (0.3% agar) (Fig. 2A and B). We found that the *bifA* motility defect in 0.3% agar is not apparently affected by the *motA* mariner mutation (Fig. 2A), indicating that this motility defect of the Δ*bifA* mutant is not obviously suppressed by mutation of the *motA* gene. Furthermore, as shown in Fig. 1A (middle row), the Δ*bifA motA*::Mar mutant shows no difference in CR binding relative to the Δ*bifA* mutant, suggesting that mutating the *motA* gene does not noticeably alter polysaccharide production under these assay conditions. In contrast, *mariner* disruption of the *motA* gene diminishes the hyperbiofilm formation phenotype of the Δ*bifA* mutant (Fig. 1A, bottom row and graph), reducing biofilm formation to a level that is not significantly different from that of the wild-type strain. Together, these data indicate that mutation of *motA* leads to restoration of swarming motility by the Δ*bifA* mutant in a manner independent of changes in swimming motility, as assayed on 0.3% soft-agar plates, or in polysaccharide production.

To further confirm these phenotypes and rule out the possibility of secondary mutations from the *mariner* insertion, we generated an in-frame deletion of the *motA* gene in the Δ*bifA* mutant background and observed the same suppression of the *bifA* mutant swarming and biofilm phenotypes as for the *mariner* mutants (Fig. 1A, compare third and fourth columns). As was the case for the transposon mutation, deletion of the *motA* gene does not suppress the soft-agar motility defect of the Δ*bifA* mutant (Fig. 2A and B).

Thus far, our data suggest that MotA participates in the repression of swarming in the Δ*bifA* mutant. In the *P. aeruginosa* PA14 genome, the *motA* gene resides in a predicted operon with the *motB* gene (PA14_65430), which in all bacterial species studied so far encodes a second component of the flagellar stator. Studies in *E. coli* have established that the flagellar stator is comprised of MotA-MotB complexes, with stoichiometry of 4MotA:2MotB and a maximum number of 11 such complexes per rotor, at high torque, forming a peptidoglycan anchored ring in the inner membrane around the core rotor proteins (44, 46–50).

Given the genomic arrangement of these genes and functional partnership of their encoded products, we sought to identify the role that each of these genes might play in the repression of swarming in the Δ*bifA* mutant. To ensure that the in-frame deletion of *motA* did not also disrupt *motB* function, we performed a complementation test of the *motA* defect in the Δ*bifA* Δ*motA* double mutant by replacing the *motA* deletion allele with the wild-type *motA* allele in the Δ*bifA* Δ*motA* strain via allelic exchange, generating the Δ*bifA* Δ*motA*::*motA* strain. As shown in Fig. 1A, the Δ*bifA* Δ*motA*::*motA* strain exhibits a swarming defect and a hyperbiofilm phenotype that are indistinguishable from those of the Δ*bifA* single mutant, indicating that introduction of the wild-type *motA* allele into the Δ*bifA* Δ*motA* double mutant fully restores the Δ*bifA* single mutant phenotypes. These results confirm that MotA plays a role in swarming inhibition in the Δ*bifA* mutant.

We next tested whether MotB also played a role in swarming inhibition by generating an in-frame deletion of the *motB* gene followed by complementation with a His_6 epitope-tagged version of *motB* on a multicopy plasmid (pMotB-His). Results indicate that deletion of *motB* in the Δ*bifA* mutant background showed similar suppression of the Δ*bifA* mutant phenotypes as observed when *motA* was mutated (Fig. 3A). Furthermore, complementation with pMotB-His fully restored the Δ*bifA* single mutant phenotypes, indicating that MotB also participates in swarming inhibition in the Δ*bifA* mutant (Fig. 3A). As was the case for mutation of the *motA* gene, deletion of the *motB* gene does not suppress the motility defect of the Δ*bifA* mutant in the soft-agar assay (Fig. 2B and 3B). Examination of a Δ*bifA* Δ*motAB* triple mutant showed that this strain has phenotypes similar to that of either the Δ*bifA* Δ*motA* or Δ*bifA* Δ*motB* double mutant (Fig. 1A, 2A and B, and 3) and confirmed that MotA and MotB participate together in repression of swarming in the Δ*bifA* mutant.

Finally, we generated single *motA* and *motB* deletion strains as well as a double *motAB* deletion strain in an otherwise wild-type background to further examine the role these stator components play in regulating motility. The Δ*motA*, Δ*motB*, and Δ*motAB* strains all showed increased swarming motility. For example, the Δ*motA* mutant showed an ~2.5-fold increase in percent surface coverage of the swarm plate relative to the wild-type strain (Fig. 1A

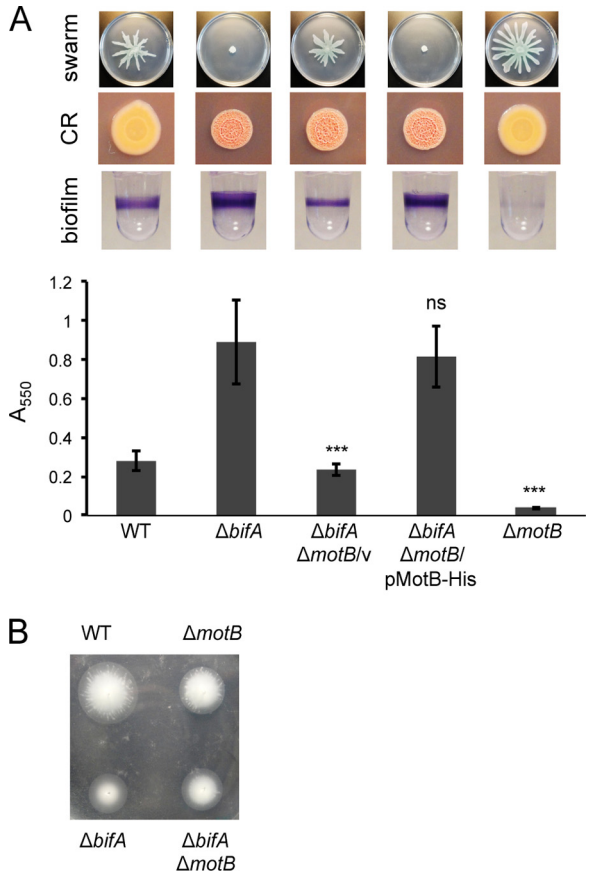

FIG 3 Assessment of *motB* mutation on suppression of *bifA* mutant phenotypes. (A) The genotype for each strain tested in this panel is shown on the *x* axis of the graph. The top row shows representative images of swarm assays for the indicated strains. Swarm plates were incubated at 37°C for 16 h. The second row shows CR binding for each strain. CR plates were incubated at 37°C for 24 h followed by 48 h of incubation at room temperature. The bottom row shows images of wells from a 96-well biofilm assay plate. The graph depicts quantification of CV-stained biofilms. Error bars indicate standard deviations of the averages from three experiments with four replicates per experiment. Data were analyzed by one-way ANOVA followed by Tukey's posttest comparison. ns, not significantly different; ***, $P < 0.001$ (relative to the Δ*bifA* mutant). (B) Representative soft-agar motility assay for the indicated strains. Plates (0.3% agar) were incubated at 37°C for 16 h.

and B). Additionally, we showed that this hyperswarming phenotype can be complemented by allelic replacement of the *motA* deletion allele with a wild-type *motA* allele (Fig. 1A, compare the wild type [WT] to the Δ*motA*::*motA* strain). Furthermore, each of these Δ*motA*, Δ*motB*, and Δ*motAB* mutant strains was able to move in the standard soft-agar (0.3% agar) motility assay, albeit at approximately 60% the level of the wild type (Fig. 1C, 2C, and 3B). These results indicate that the MotAB stator likely plays a positive but relatively minor role in motility under the soft-agar assay conditions studied here; however, this stator has a measurable negative impact on swarming motility, even when c-di-GMP levels are relatively low in the WT strain (compared to elevated conditions observed for the Δ*bifA* mutant). Taken together, our data indicate that the role of MotAB in repressing swarming motility is not specific to the Δ*bifA* mutant, as we observe similar negative impacts on swarming in the WT.

Based on the observations that the MotAB stator negatively impacts swarming, we assessed whether overexpression of a His_6 epitope-tagged version of *motA* from a multicopy plasmid (pMotA-His) under the control of the arabinose-inducible pBAD promoter in the wild-type strain would lead to repression of swarming, and that is indeed what we observed (Fig. 1D). However, overexpression of the pMotB-His plasmid alone did not repress swarming in the wild type (data not shown). These data suggest that MotA may play a specific role in repression of swarming; possible explanations include that only MotA and not MotB can be incorporated into the stator when overexpressed or, alternatively, that MotB incorporation into the stator requires MotA and that assembly of MotB into the motor is necessary for its repressive function. Recent studies in *Salmonella* support the notion that overexpression of MotA alone can lead to its incorporation into the motor, with subsequent deleterious effects on motility (51).

***P. aeruginosa* has two stators sets with distinct and opposing roles in motility.** Despite the fact that *P. aeruginosa* builds a single polar flagellum, its genome encodes two flagellar stator sets, MotAB (as described above) and MotCD (PA14_45560/45540) (52–54). In contrast, *E. coli* and *Salmonella enterica*, both well-studied model organisms for flagellar structure and function, build multiple flagella per cell (i.e., they are peritrichous), but the genomes of these microbes encode only a single MotAB stator set. As outlined above, our data suggest that the MotAB stator has a negative impact on swarming motility under wild-type conditions as well as when c-di-GMP levels are highly elevated (i.e., in the Δ*bifA* mutant).

In contrast, the single Δ*motC* and Δ*motCD* double mutant strains exhibit complete loss of swarming motility and are indistinguishable from the Δ*flgK* nonmotile control (Fig. 1B; also, see Fig. S1A in the supplemental material), indicating that the MotCD stator is critical for swarming motility under these conditions. In soft-agar motility assays, the Δ*motC* and Δ*motCD* mutants exhibit a very small but detectable swim zone that is typically less than 5% of that of the wild type and that is absent in the Δ*flgK* mutant (Fig. 1C; also, see Fig. S1B in the supplemental material). These results are consistent with MotCD being the predominant stator required for swimming motility in addition to its critical role in swarming. However, taken together with the observation that Δ*motAB* mutants also exhibit a modest decrease in swimming, our data suggest that swimming motility under these conditions is optimal when both MotAB and MotCD stators are present. Given that a stator is comprised of multiple Mot protein complexes, with up to 11 MotAB complexes in *E. coli* (49), we infer from these data that MotAB and MotCD complexes could both be present in the stator of a given flagellar motor.

Discrepancy between findings here and in a previous study from our group. In earlier work from our group, we reported that the Δ*motCD* mutant was able to swim as well as the wild type and the Δ*motAB* mutant on 0.3% agar plates and that the *motCD* mutant was also able to swarm on plates solidified with 0.45% agar but not on 0.5% agar plates (53). In this study, we observed very little swimming and no swarming on either 0.45% or 0.5% agar plates by the Δ*motC* or Δ*motCD* mutants (Fig. 1B and C; also, see Fig. S1 in the supplemental material), findings that are similar to those reported for *P. aeruginosa* strain PAO1 (54). The exact cause of the discrepancies between the earlier and current study is not clear, but one possibility is that the Δ*motCD* mutant became con-

taminated with wild-type cells at some point during experimentation in the earlier study.

For the current study, the Δ*motCD* deletion strain was reconstructed, and additionally, an individual Δ*motC* deletion mutant was built for a more thorough phenotypic characterization of the Δ*motCD* locus. Here we show that the newly generated Δ*motCD* and Δ*motC* deletion strains are phenotypically indistinguishable from one another, and we further show complementation of the Δ*motC* strain using a His_6 epitope-tagged version of Δ*motC* on a multicopy plasmid (pMotC-His) to restore swimming and partially restore swarming to this mutant (see Fig. S1 in the supplemental material). Thus, we feel confident that the current study provides a more accurate assessment of the role that MotCD plays in motility. Taken together, the data in the current study suggest that the stator sets of *P. aeruginosa*, MotAB and MotCD, have distinct roles in controlling motility and most notably, as described above, have opposite roles in impacting swarming motility in particular.

c-di-GMP levels do not impact MotA and -C protein levels or subcellular localization. Given that the MotAB stator is required for robust repression of swarming when c-di-GMP levels are elevated, we hypothesized that c-di-GMP levels might influence the abundance and/or subcellular localization of MotAB or MotCD in cells. To address this possibility, we constructed epitope-tagged versions of either *motA* or *motC* at their native loci on the chromosome in either the wild-type or *bifA* mutant backgrounds (*motA*$^+$-His, Δ*bifA motA*$^+$-His, *motC*$^+$-HA, and Δ*bifA motC*$^+$-HA). It should be noted that the His_6 epitope tag had no impact on MotA function in either the wild-type or Δ*bifA* mutant strain (see below). However, given the critical role of MotC in swimming and swarming motility, we did observe that the HA epitope tag led to a moderate reduction in swimming by both the wild-type and Δ*bifA* mutant strains, as well as a strong reduction in swarming by the wild type (data not shown).

We next fractionated (swarm) surface-grown cells and probed for the presence of these proteins in various cellular fractions. In the wild-type strain backgrounds, we detected both the MotA-His and MotC-HA proteins predominantly in the total membrane (TM) and inner membrane (IM) fractions but not in the cytosolic or outer membrane fractions (Fig. 4), which is consistent with the cellular organization of the stator proteins in the flagellum from studies in *E. coli* (47, 48). We found no obvious changes in the localization pattern of either MotA-His or MotC-HA in the Δ*bifA* mutant cells relative to wild-type cells in any of the fractions, nor did we observe any obvious differences in the levels of these two proteins when comparing these strains.

To confirm that MotA protein levels do not increase with c-di-GMP levels, we quantified MotA-His protein levels in whole-cell-lysate samples for each strain by Western blotting and found no significant difference between the two strains (measured as integrated pixel density × 10^4: the WT value was 21.5 ± 1.9, whereas that for the *bifA* strain was 19.2 ± 3.8 [$P = 0.29$ by *t* test; three independent experiments, with three replicates per strain]). Together these data argue against a simple model wherein c-di-GMP levels alter motility by controlling expression levels or membrane localization of either MotA or MotC.

MotA-FliG interactions are important for repression of swarming. While the precise mechanism by which the Mot proteins are assembled into the stator of the flagellum is not well understood, genetic studies in *E. coli* and *S. enterica* have indicated

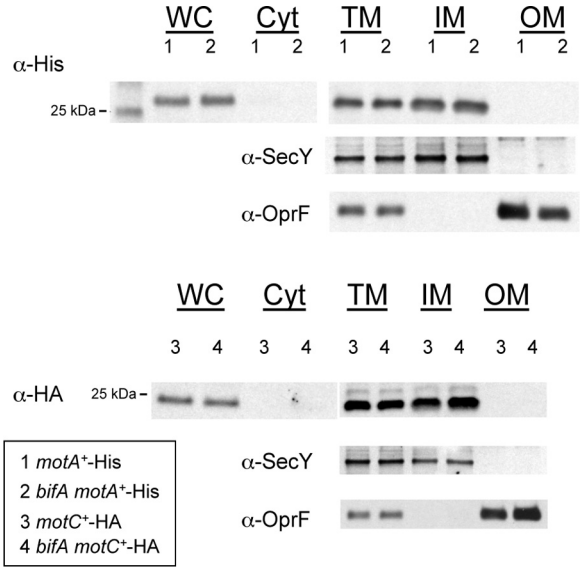

FIG 4 Subcellular fractionation and level of MotA-His and MotC-HA. Cellular fractions of swarm-grown cells of the *motA*$^+$-His and Δ*bifA motA*$^+$-His strains (top) and *motC*$^+$-HA, and Δ*bifA motC*$^+$-HA strains (bottom) were separated on 12% SDS-PAGE gels. Fractions are indicated as whole cell (WC), soluble cytoplasmic (Cyt), total membrane (TM), inner membrane (IM), and outer membrane (OM). Lanes are labeled according to the legend in the lower left corner. Western analysis was performed using the following antibodies, as indicated: anti-His (for MotA-His), anti-HA (for MotC-HA), anti-SecY, and anti-OprF. SecY and OprF serve as controls for integrity of inner and outer membrane fractions, respectively.

that specific interactions between MotA and the FliG rotor protein are important not only for rotation of the flagellum but also for assembly of MotA into the motor (51, 55–57). The rotor/stator interface involves a small number of highly conserved amino acids in each protein, the main feature of which is their charge, as these interactions are believed to be largely electrostatic (56–58).

Extensive mutational analyses have been used to define the MotA-FliG interface (56–58). In MotA, an arginine at position 90 (R90) and a glutamic acid at position 98 (E98) have been shown to be important in interacting with D289 and R281, respectively, of FliG. For example, mutation of MotA R90 to E (R90E) reverses the positive charge to negative and leads to full inhibition of motility, whereas compensatory mutation of FliG D289 to A (neutral) or K (positive) in the *motA*(R90E) strain partially suppresses this motility defect. Furthermore, additional studies from Morimoto et al. indicate that the MotA R90/FliG D289 interaction may play a more important role in stator assembly, while the MotA E98/FliG R281 interaction appears to be more influential in torque generation (55).

Given that the R90 and E98 residues of MotA and D289 and R281 of FliG are conserved in the respective *P. aeruginosa* proteins, we tested whether MotA-FliG interactions might be important for the participation of MotA in repression of swarming. To this end, we generated a C-terminal His_6 epitope tag in the *motA* gene at its native locus on the chromosome in either the wild-type or the Δ*bifA* background. As mentioned above, the His_6 epitope tag had no impact on MotA function in either the wild-type or Δ*bifA* mutant strain (Fig. 5, compare to Fig. 1). We then introduced the substitutions to generate R90E or E98K variations in this chromosomal *motA* locus encoding MotA-His. First, we ex-

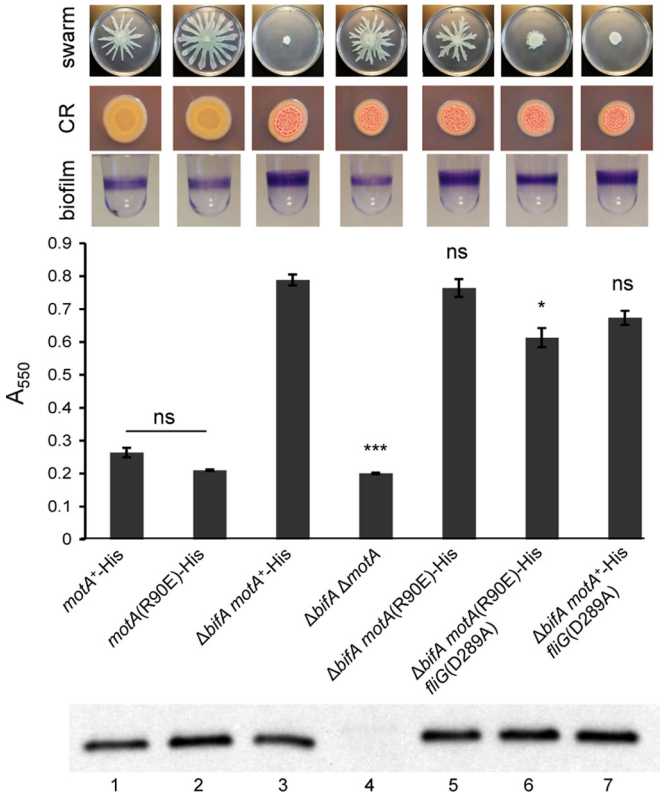

FIG 5 Assessment of the role MotA-FliG interactions play in swarming inhibition. The strain genotype for each strain tested in this panel is shown on the *x* axis of the graph. The top row shows representative swarm images for the indicated strains. Swarm plates were incubated at 37°C for 16 h. The second row shows CR binding for each strain. CR assay plates were incubated at 37°C for 24 h, followed by 48 h at room temperature. The bottom row shows images of wells from a representative 96-well biofilm assay plate. Strains were grown in M63 medium supplement with glucose, $MgSO_4$, and CAA for 24 h prior to crystal violet (CV) staining. The graph depicts quantification of CV-stained biofilms. CV was solubilized in 30% glacial acetic acid and the absorbance was read at 550 nm. Error bars indicate standard deviations of the average of three experiments with four replicates per experiment. Data were analyzed by one-way ANOVA followed by Tukey's posttest comparison. ns, not significantly different; *, $P < 0.05$; ***, $P < 0.001$ (all relative to the Δ*bifA motA*$^+$-His strain, except where indicated). The bottom panel shows a representative Western blot assessing chromosomally expressed MotA-His and MotA(R90E)-His protein levels in strains with the indicated genotypes. Lanes: 1, *motA*$^+$-His; 2, *motA*(R90E)-His; 3, Δ*bifA motA*$^+$-His; 4, Δ*bifA* Δ*motA*; 5, Δ*bifA motA*(R90E)-His; 6, Δ*bifA motA*(R90E)-His *fliG*(D289A); 7, Δ*bifA motA*$^+$-His *fliG*(D289A). Equal amounts of total protein from whole-cell lysates prepared from each strain were resolved by SDS-PAGE on a 12% polyacrylamide gel. The His_6 epitope-tagged proteins were detected using an anti-penta-His antibody.

amined protein levels in cells cultured on a swarm agar surface and found that the MotA(R90E)-His and MotA(E98K)-His mutant proteins are present at levels comparable to that of wild-type MotA-His (Fig. 5 and Fig. S2 in the supplemental material, respectively).

If the MotA-FliG interaction is important for repression of swarming, then we would predict that the R90E and E98K mutations would disrupt this interaction, thereby leading to increased swarming, particularly in the Δ*bifA* mutant background. Indeed, this is what we observed (Fig. 5; also, see Fig. S2 in the supplemental material). Both the Δ*bifA motA*(R90E)-His and Δ*bifA motA*(E98K)-His strains exhibited recovery of swarming motility comparable to that of the Δ*bifA* Δ*motA* deletion strain, suggesting that these mutations largely disrupt function of MotA in repressing swarming.

Interestingly, however, the R90E substitution shows virtually no effect on the hyperbiofilm phenotype of the Δ*bifA* mutant, in contrast to the substantial reduction in biofilm formation observed for the Δ*bifA motA*(E98K)-His strain (see Fig. S2 in the supplemental material), which more closely resembles the Δ*bifA* Δ*motA* strain in this regard. Thus, the R90E mutation appears to specifically impair the ability of MotA to participate in swarming repression but not in biofilm formation, thereby separating these as two distinct functions of MotA. This notion is further supported by the *motA*(R90E)-His single mutant strain, which exhibits increased swarming relative to the wild type {surface coverage = 20% ± 4% [WT] and 52% ± 8% [*motA*(R90E)]} but has no significant impact on biofilm formation (Fig. 5, first and second columns on the left). In contrast, the *motA*(E98K)-His single mutant strain shows increased swarming relative to the wild type but shows a significant reduction in biofilm formation (see Fig. S2 in the supplemental material). It is unclear why the R90E mutation has no impact on biofilm formation, but it seems unlikely that this distinction could be explained simply by differences in swimming motility or CR binding given that there are no obvious phenotypic differences between the *motA*(R90E)-His and *motA*(E98K)-His strains and the *motA* deletion strain in either the wild-type or Δ*bifA* mutant background in these assays (Fig. 5; also, see Fig. S2 and S3 in the supplemental material). Furthermore, the observation that the *motA*(R90E)-His and *motA*(E98K)-His mutations in the WT background also result in enhancement of swarming (Fig. 5; also, see Fig. S2, top; compare to the *motA*$^+$-His strain) suggests that the observed effects of these *motA* point mutations on swarming are not specific to the Δ*bifA* mutant background.

To further probe whether the MotA-FliG interaction is important for swarming repression, we sought to introduce a compensatory *fliG* mutation into either the Δ*bifA motA*(R90E)-His or Δ*bifA motA*(E98K)-His strain; based on the studies in *E. coli* and *Salmonella*, this mutation would be expected to restore interaction of FliG with the mutant version of MotA. If our hypothesis is correct, then restoration of the interaction between these variant proteins in the Δ*bifA* mutant background should restore swarming inhibition. One additional but important consideration, in our case, was that the FliG-MotC interaction presumably must be maintained for swarming motility to occur based on the essential role for MotC particularly in swarming motility (see above). If this interaction was disrupted, then we could not properly evaluate the impact of a *fliG* mutation on the Δ*bifA motA*(R90E)-His or Δ*bifA motA*(E98K)-His strain.

Given that the R90 and E98 residues of MotA are also conserved in MotC, we surmised that interaction of MotC with FliG would occur via the same electrostatic interactions. Thus, we chose the *fliG*(D289A) substitution that in *E. coli* acted as an allele-specific suppressor of the *motA*(R90E) nonmotile mutant (restored ~40% of wild-type motility) with little impact on motility in a *motA*$^+$ background (exhibits ~92% of wild-type motility). In contrast, *fliG*(R281V) or *fliG*(R281W) single mutations which act as allele-specific suppressors of the *motA*(E98K) mutant led to loss of motility and would be predicted to negatively impact the FliG/MotC interaction.

In *P. aeruginosa*, the *motA*$^+$-His *fliG*(D289A) strain showed a modest decrease (~20% reduction) in motility in the soft-agar

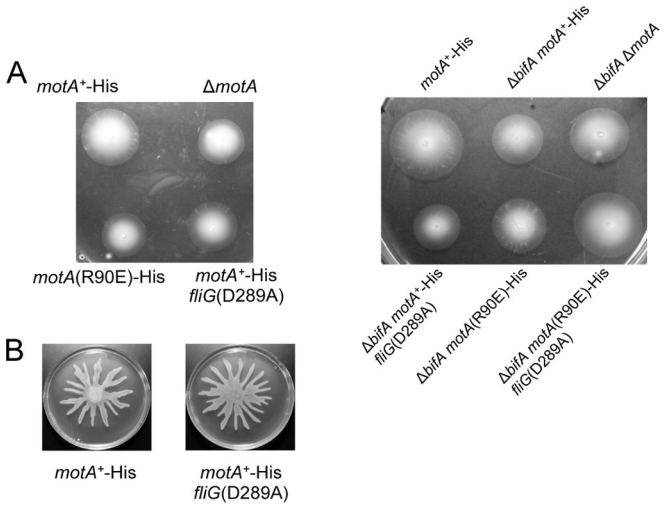

FIG 6 Motility assays to assess the impact of *motA* and *fliG* mutations. Images show representative motility in 0.3% soft-agar motility (A) and swarm (B) assays for strains with the indicated genotypes.

assay relative to the *motA*$^+$-His parent strain (Fig. 6A). However, this strain did not exhibit an obvious defect in swarming motility (Fig. 6B), nor was there a significant difference in biofilm formation (data not shown). It is unclear why the *fliG*(D289A) mutation has an impact on swimming but not swarming motility; however, based on these phenotypes, we concluded that MotCD function is not significantly impaired by this *fliG* mutation.

Introduction of the *fliG*(D289A) mutation into the Δ*bifA motA*$^+$-His strain had little impact on the Δ*bifA* mutant phenotypes, save for a modest reduction in biofilm formation (Fig. 5). Swarming motility remained inhibited (Fig. 5), indicating that mutation of *fliG* alone did not disrupt the ability of MotA to repress swarming. However, introducing the *fliG*(D289A) mutation into the Δ*bifA motA*(R90E)-His strain led to a marked reduction in swarming motility relative to the robust swarming observed for the Δ*bifA motA*(R90E)-His strain alone; more specifically, the Δ*bifA motA*(R90E)-His *fliG*(D289A) strain showed severely reduced tendril formation (Fig. 5). Thus, while the triple mutant strain is not identical to the Δ*bifA* single mutant in terms of full swarming inhibition, the observed reduction in swarming motility suggests that the compensatory *fliG*(D289A) mutation does restore some measure of swarming inhibition to the Δ*bifA motA*(R90E)-His mutant, as predicted.

In contrast to the swarming phenotype, there is no negative impact on swimming motility of this triple Δ*bifA motA*(R90E)-His *fliG*(D289A) mutant relative to either of the double mutants alone, supporting the notion that these mutations together do not impair MotCD function (Fig. 6; also, see Fig. S3 in the supplemental material). Taken together, these data support the hypothesis that repression of swarming by MotA relies upon an interaction with FliG, which, based upon the studies in *E. coli* and *Salmonella*, likely influences assembly of MotA into the stator.

Elevated c-di-GMP levels impact polar localization of GFP-MotD but not GFP-MotB. Thus far, our data suggest that the different stator complexes of *P. aeruginosa*, MotAB and MotCD, play distinct roles in regulating swarming motility. That is, the MotCD complex is required for swarming motility, while the MotAB stator complex contributes to the repression of swarming motility in the wild type as well as in the Δ*bifA* mutant, where c-di-GMP levels are elevated. Furthermore, the ability of MotAB to repress swarming depends upon interaction of MotA with FliG in the motor, suggesting that repression by MotAB may require incorporation of this stator complex into the motor.

Together these data lead us to hypothesize that c-di-GMP levels might impact stator composition at the flagellar motor. In support of this hypothesis, it is known that stators in functioning motors exchange with stators diffusing in the membrane (without requiring disassembly and reassembly of the transmembrane rotor components of the motor) and that such exchanges could occur rapidly enough to allow cells to respond to changing c-di-GMP levels (39, 59, 60).

To assess whether c-di-GMP levels affect localization of the stator components, we replaced *motB* and *motD* genes with *gfp-motB* and *gfp-motD*, respectively, at their native chromosomal loci so that expression would occur similarly to that in their wild-type counterparts. When they were assessed in swarming assays, we found that the *gfp-motB* and *gfp-motD* strains swarmed comparably to the wild-type parental strain (see Fig. S4A in the supplemental material), indicating that the *gfp* fusions did not noticeably impact function of either MotB or MotD. Furthermore, the *gfp-motB* fusion had little impact on the Δ*bifA* swarming-defective strain, indicating no significant loss of *motB* repressive function (see Fig. S4B in the supplemental material).

Using fluorescence microscopy, we analyzed the localization of the GFP-labeled stator units in bacteria grown on the surface under conditions identical to those used in our swarming motility assays. For each strain, mobile and static bright spots (or puncta) of fluorescence were observed, although with different patterns depending on the strain. For each field of view imaged, we counted the total number of cells and the number of cells showing a polar fluorescent spot to assess whether c-di-GMP level affected polar localization of either of the GFP-labeled stator units.

For GFP-MotB, we saw no differential polar localization of the GFP-MotB fusion protein in the wild type compared to any of the other mutants analyzed, including the Δ*bifA* mutant, the Δ*bifA motA*(R90E) or Δ*bifA fliG*(D289A) double mutant, or the Δ*bifA motA*(R90E) *fliG*(D289A) triple mutant (Fig. 7A). These data indicate that the polar localization of GFP-MotB is not noticeably affected by c-di-GMP level or by alterations in MotA-FliG interactions. Furthermore, there was also no difference in GFP-MotB polar localization in the Δ*motCD* deletion mutant relative to the wild type (Fig. 7A), suggesting that polar localization of GFP-MotB is not detectably influenced by the presence or absence of MotCD. However, we cannot rule out the possibility that more subtle changes in MotB localization do occur.

In contrast, we did observe changes in GFP-MotD localization. Shown in Fig. 7B are representative images of cells expressing the GFP-MotD fusion protein. In the wild-type genetic background, the GFP-MotD puncta were observed at the pole as well as in other locations on the periphery of the cells, consistent with the known membrane localization of stator components. Interestingly, the percentage of cells with polar puncta for GFP-MotD (~25%) was less than that observed for GFP-MotB (~45%) (Fig. 7A and C). The significance of this difference is not clear.

Under conditions of high c-di-GMP in the Δ*bifA* mutant background, there were fewer distinct GFP-MotD puncta in these cells compared to the WT (Fig. 7B). When we quantified the percentage of cells showing a polar fluorescent spot, we found that there

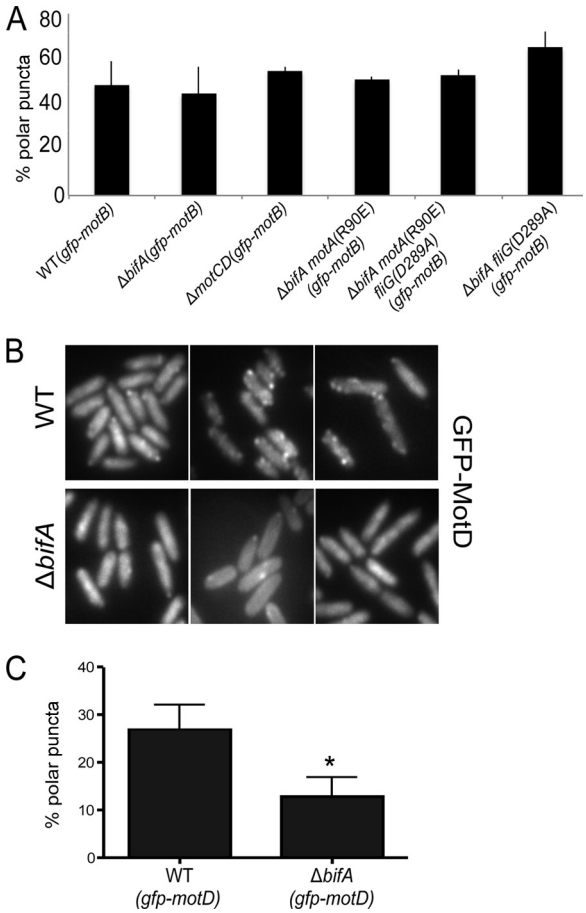

FIG 7 High c-di-GMP alters the localization of GFP-MotD, as assessed by fluorescence microscopy. (A) Percentage of cells showing polar puncta of GFP-MotB plotted for the strains indicated. There are no discernible differences among any of these strains tested (2 replicate experiments per strain tested). (B) Representative images of the WT and Δ*bifA* mutant strains expressing GFP-MotD from the chromosome. (C) The percentage of cells with GFP-MotD polar puncta is plotted for the wild type (WT) and the Δ*bifA* mutant. Three independent replicate experiments were performed per strain, with an average of at least 200 total cells counted per experiment. *, significantly different, as judged by a *t* test ($P < 0.05$).

was a significant reduction of the GFP-MotD puncta at cell poles in the Δ*bifA* mutant relative to the wild type (Fig. 7C). These data suggest that an elevated c-di-GMP level does impact localization of MotD at the cell pole, with fewer GFP-MotD puncta in the Δ*bifA* mutant, a strain that lacks swarming motility.

DISCUSSION

Our work here is consistent with the identification of a new mechanism for c-di-GMP-mediated regulation. That is, we propose that c-di-GMP can impact regulation of swarming motility, likely via the differential utilization of the two sets of stators present in *P. aeruginosa*. It is clear that swimming motility in organisms with a single stator system (i.e., *E. coli* and *S. enterica*) is also c-di-GMP regulated, but for these organisms, control appears to be at the level of regulating the single stator function and/or its interaction with the motor (15, 16, 18). Here we propose that the two stators play discrete roles in the regulation of swarming motility. MotCD appears to be the major torque-generating stator, as mutating the *motCD* genes results in loss of swarming. In contrast, loss of MotAB results in a hyperswarming phenotype, while overexpression of MotA fully represses swarming.

We also showed using a genetic approach that interactions between MotA and FliG are critical for MotA-mediated suppression of swarming, indicating that this stator component functions in repression by occupying the motor in a mechanism analogous to that characterized in *E. coli* and *S. enterica* (51, 57). As a follow-up to these studies, using a bacterial two-hybrid analysis, we explored whether the mutations we generated in MotA and FliG do indeed impact MotA-FliG interactions. We were unable to detect any evidence for MotA-FliG interactions using a variety of different construct combinations (data not shown); however, these interactions have not been demonstrated for other species and are considered unlikely given the transient, electrostatic nature of the stator/rotor interaction.

Overall, our data suggest that differential occupancy of the motor by the MotAB versus MotCD stators may impact swarming motility. Such a model would suggest that stators must exchange in the motor in response to differential environmental signals. Two key studies in *E. coli* provide strong evidence for stator exchange. Both studies examined stator incorporation into functioning flagellar motors in real time and led to the discovery that stator assembly is a remarkably dynamic process. An early study showed that stator components of *E. coli* could be added to an otherwise assembled but nonrotating flagellum of a *mot* mutant (tethered by its flagellum) by inducing expression of the *motAB* genes on a plasmid, leading to discrete stepwise increases in the speed of flagellar rotation, with each step corresponding to the addition of a new stator complex (59). These results established not only that stator complexes could be added as the last component to the flagellum (i.e., flagellar assembly was not dependent upon stator incorporation) but also that stator complexes could be added while the flagellum was actually rotating. A more recent study used total internal reflection fluorescence (TIRF) microscopy to track the movement of GFP-MotB molecules into and out of the stator of *E. coli* cells tethered by their flagellar filaments (39). This study found that GFP-MotB (presumably in complex with its MotA partner) undergoes a process of stator exchange whereby this molecule shuttles between an inner membrane pool of ~200 GFP-MotB molecules and the stator of the motor, with a given GFP-MotB molecule having an average residence time in the stator of only ~30 s. Moreover, recent studies showed that the number of stators engaged in a motor at any one time also may change as the external force on the flagellum changes. For example, the number of stators engaged in a motor increases with increasing external forces, as would occur with increasing viscosity, such as on swarm agar or at a surface during biofilm formation (50, 61), suggesting a structural change within the rotor that retains stators and allows increased torque.

Additional evidence for stator exchange comes from studies in *Shewanella*, an organism with both proton-driven and sodium-driven stator sets powering a single polar flagellum. *Shewanella oneidensis* has been shown to preferentially use one stator set over the other depending on environmental conditions (60), thus providing an additional precedent for more than one stator functioning in the same motor.

At this point, the mechanism by which the cell employs c-di-GMP to control stator utilization is not clear. Our findings show that high c-di-GMP level is associated with a decrease in polar

localization of GFP-MotD. Thus, it is possible that c-di-GMP drives relocalization of the MotCD stator away from the pole; however, we cannot rule out the possibility that additional mechanisms contribute to this decrease in polar-localized MotD. It is important to note that we used a mutant strain in these localization studies (the Δ*bifA* mutant), and thus, we may need to identify more physiologically relevant conditions for high c-di-GMP levels to better understand this localization phenomenon. We reported previously that c-di-GMP levels are elevated when *P. aeruginosa* is grown on a surface versus planktonically (37). However, comparing planktonically versus surface-grown cells to mimic a physiological increase in c-di-GMP levels is complicated by the fact that to image planktonically grown cells, one must place them on a surface. Future studies might be aided by using fixed cells grown under these different conditions. In contrast to the MotCD stator, the MotAB stator set, as judged by GFP-MotB localization, seems largely unresponsive to c-di-GMP levels or any other condition tested in this study regarding its polar localization. Thus, our current data are consistent with a model whereby c-di-GMP likely controls occupancy of the motor by the different stator sets primarily by shifting localization of MotCD.

Previous studies identified a role for PilZ-like proteins in the control of flagellar function, for example, the YcgR protein in *E. coli*, although the precise mechanism of this control is still controversial (2, 14–16, 18). *P. aeruginosa* PA14 has 8 PilZ-like proteins, including one protein with high sequence similarity to YcgR, and we are currently exploring which of these proteins might contribute to c-di-GMP-mediated swarming regulation via the stators.

In summary, our data are consistent with a model wherein *P. aeruginosa* uses two distinct stator sets to control surface motility in response to c-di-GMP. The novelty of these findings indicates that there are likely still other, as-yet-unidentified c-di-GMP outputs to uncover and highlights the complexity and adaptability of this signaling network. Furthermore, analyses of bacterial genomic sequence data indicate that in addition to *P. aeruginosa*, microbes with a single flagellar motor that possess two or more stator sets are surprisingly common and widespread across bacterial species (53, 62). Thus, it is possible that our findings may be extended to these other organisms with two stator sets, such as species of *Xanthomonas* and *Burkholderia*, as well as *Yersinia pestis* and *Chromobacterium violaceum* (53, 62); however, we cannot rule out the possibility that the dual stators play roles other than c-di-GMP-mediated motility control in these different organisms.

ACKNOWLEDGMENTS

This work was supported by NIH grant R01 2 R37 AI83256-06 to G.A.O. and BBSRC and EPA Cephalosporin funding to J.P.A. L.M.F. was supported by the Renal Function and Disease Training Grant (T32 DK007301) and award T32 GM008704 from the National Institute of General Medical Sciences.

REFERENCES

1. **Ross P, Weinhouse H, Aloni Y, Michaeli D, Weinberger-Ohana P, Mayer R, Braun S, de Vroom E, van der Marel GA, van Boom JH, Benziman M.** 1987. Regulation of cellulose synthesis in *Acetobacter xylinum* by cyclic diguanylic acid. Nature **325:**279–281. http://dx.doi.org/10.1038/325279a0.
2. **Boyd CD, O'Toole GA.** 2012. Second messenger regulation of biofilm formation: breakthroughs in understanding c-di-GMP effector systems. Annu Rev Cell Dev Biol **28:**439–462. http://dx.doi.org/10.1146/annurev-cellbio-101011-155705.
3. **Hengge R.** 2009. Principles of c-di-GMP signalling in bacteria. Nat Rev Microbiology **7:**263–273. http://dx.doi.org/10.1038/nrmicro2109.
4. **Römling U, Galperin M, Gomelsky M.** 2013. Cyclic di-GMP: the first 25 years of a universal bacterial second messenger. Microbiol Mol Biol Rev **77:**1–52. http://dx.doi.org/10.1128/MMBR.00043-12.
5. **Jenal U.** 2004. Cyclic di-guanosine-monophosphate comes of age: a novel secondary messenger involved in modulating cell surface structures in bacteria? Curr Opin Microbiol **7:**185–191. http://dx.doi.org/10.1016/j.mib.2004.02.007.
6. **Simm R, Morr M, Kader A, Nimtz M, Romling U.** 2004. GGDEF and EAL domains inversely regulate cyclic di-GMP levels and transition from sessility to motility. Mol Microbiol **53:**1123–1134. http://dx.doi.org/10.1111/j.1365-2958.2004.04206.x.
7. **Christen M, Christen B, Folcher M, Schauerte A, Jenal U.** 2005. Identification and characterization of a cyclic di-GMP-specific phosphodiesterase and its allosteric control by GTP. J Biol Chem **280:**30829–30837. http://dx.doi.org/10.1074/jbc.M504429200.
8. **Paul R, Weiser S, Amiot NC, Chan C, Schirmer T, Giese B, Jenal U.** 2004. Cell cycle-dependent dynamic localization of a bacterial response regulator with a novel di-guanylate cyclase output domain. Genes Dev **18:**715–727. http://dx.doi.org/10.1101/gad.289504.
9. **Ryan RP, Fouhy Y, Lucey J F, Crossman LC, Spiro S, He YW, Zhang LH, Heeb S, Camara M, Williams P, Dow JM.** 2006. Cell-cell signaling in *Xanthomonas campestris* involves an HD-GYP domain protein that functions in cyclic di-GMP turnover. Proc Natl Acad Sci U S A **103:**6712–6717. http://dx.doi.org/10.1073/pnas.0600345103.
10. **Schirmer T, Jenal U.** 2009. Structural and mechanistic determinants of c-di-GMP signalling. Nat Rev Microbiol **7:**724–735. http://dx.doi.org/10.1038/nrmicro2203.
11. **Tischler AD, Camilli A.** 2004. Cyclic diguanylate (c-di-GMP) regulates *Vibrio cholerae* biofilm formation. Mol Microbiol **53:**857–869. http://dx.doi.org/10.1111/j.1365-2958.2004.04155.x.
12. **Sondermann H, Shikuma NJ, Yildiz FH.** 2012. You've come a long way: c-di-GMP signaling. Curr Opin Microbiol **15:**140–146. http://dx.doi.org/10.1016/j.mib.2011.12.008.
13. **Amikam D, Galperin MY.** 2006. PilZ domain is part of the bacterial c-di-GMP binding protein. Bioinformatics **22:**3–6. http://dx.doi.org/10.1093/bioinformatics/bti739.
14. **Ryjenkov DA, Simm R, Römling U, Gomelsky M.** 2006. The PilZ domain is a receptor for the second messenger c-di-GMP. The PilZ domain protein YcgR controls motility in enterobacteria. J Biol Chem **281:**30310–30314. http://dx.doi.org/10.1074/jbc.C600179200.
15. **Boehm A, Kaiser M, Li H, Spangler C, Kasper CA, Ackermann M, Kaever V, Sourjik V, Roth V, Jenal U.** 2010. Second messenger-mediated adjustment of bacterial swimming velocity. Cell **141:**107–116. http://dx.doi.org/10.1016/j.cell.2010.01.018.
16. **Fang X, Gomelsky M.** 2010. A post-translational, c-di-GMP-dependent mechanism regulating flagellar motility. Mol Microbiol **76:**1295–1305. http://dx.doi.org/10.1111/j.1365-2958.2010.07179.x.
17. **Ko M, Park C.** 2000. Two novel flagellar components and H-NS are involved in the motor function of *Escherichia coli*. J Mol Biol **303:**371–382. http://dx.doi.org/10.1006/jmbi.2000.4147.
18. **Paul K, Nieto V, Carlquist WC, Blair DF, Harshey RM.** 2010. The c-di-GMP binding protein YcgR controls flagellar motor direction and speed to affect chemotaxis by a "backstop brake" mechanism. Mol Cell **38:**128–139. http://dx.doi.org/10.1016/j.molcel.2010.03.001.
19. **Martínez-Granero F, Navazo A, Barahona E, Redondo-Nieto M, González de Heredia E, Baena I, Martín-Martín I, Rivilla R, Martín M.** 2014. Identification of *flgZ* as a flagellar gene encoding a PilZ domain protein that regulates swimming motility and biofilm formation in *Pseudomonas*. PLoS One **9:**e87608. http://dx.doi.org/10.1371/journal.pone.0087608.
20. **Brown MT, Delalez NJ, Armitage JP.** 2011. Protein dynamics and mechanisms controlling the rotational behaviour of the bacterial flagellar motor. Curr Opin Microbiol **14:**734–740. http://dx.doi.org/10.1016/j.mib.2011.09.009.
21. **Baraquet C, Murakami K, Parsek MR, Harwood CS.** 2012. The FleQ protein from *Pseudomonas aeruginosa* functions as both a repressor and an activator to control gene expression from the *pel* operon promoter in response to c-di-GMP. Nucleic Acids Res **40:**7207–7218. http://dx.doi.org/10.1093/nar/gks384.
22. **Hickman JW, Harwood CS.** 2008. Identification of FleQ from *Pseudomo-*

nas aeruginosa as a c-di-GMP-responsive transcription factor. Mol Microbiol **69:**376–389. http://dx.doi.org/10.1111/j.1365-2958.2008.06281.x.
23. **Wolfe AJ, Visick KL.** 2008. Get the message out: cyclic-di-GMP regulates multiple levels of flagellum-based motility. J Bacteriol **190:**463–475. http://dx.doi.org/10.1128/JB.01418-07.
24. **Zorraquino V, García B, Latasa C, Echeverz M, Toledo-Arana A, Valle J, Lasa I, Solano C.** 2013. Coordinated cyclic-di-GMP repression of *Salmonella* motility through YcgR and cellulose. J Bacteriol **195:**417–428. http://dx.doi.org/10.1128/JB.01789-12.
25. **Shanks RM, Caiazza NC, Hinsa SM, Toutain CM, O'Toole GA.** 2006. *Saccharomyces cerevisiae*-based molecular tool kit for manipulation of genes from gram-negative bacteria. Appl Environ Microbiol **72:**5027–5036. http://dx.doi.org/10.1128/AEM.00682-06.
26. **Hoang TT, Karkhoff-Schweizer RR, Kutchma AJ, Schweizer HP.** 1998. A broad-host-range Flp-*FRT* recombination system for site specific excision of chromosomally-located DNA sequences: application for isolation of unmarked *Pseudomonas aeruginosa* mutants. Gene **212:**77–86. http://dx.doi.org/10.1016/S0378-1119(98)00130-9.
27. **Schweizer HP.** 1992. Allelic exchange in *Pseudomonas aeruginosa* using novel ColE1-type vectors and a family of cassettes containing a portable *oriT* and the counter-selectable *Bacillus subtilis sacB* marker. Mol Microbiol **6:**1195–1204. http://dx.doi.org/10.1111/j.1365-2958.1992.tb01558.x.
28. **Ha D-G, Kuchma SL, O'Toole GA.** 2014. Plate-based assay for swimming motility in *Pseudomonas aeruginosa*. Methods Mol Biol **1149:**59–65. http://dx.doi.org/10.1007/978-1-4939-0473-0_7.
29. **Ha D-G, Kuchma SL, O'Toole GA.** 2014. Plate-based assay for swarming motility in *Pseudomonas aeruginosa*. Methods Mol Biol **1149:**67–72. http://dx.doi.org/10.1007/978-1-4939-0473-0_8.
30. **Caiazza NC, O'Toole GA.** 2004. SadB is required for the transition from reversible to irreversible attachment during biofilm formation by *Pseudomonas aeruginosa* PA14. J Bacteriol **186:**4476–4485. http://dx.doi.org/10.1128/JB.186.14.4476-4485.2004.
31. **O'Toole GA, Kolter R.** 1998. Flagellar and twitching motility are necessary for *Pseudomonas aeruginosa* biofilm development. Mol Microbiol **30:**295–304. http://dx.doi.org/10.1046/j.1365-2958.1998.01062.x.
32. **Friedman L, Kolter R.** 2004. Genes involved in matrix formation in *Pseudomonas aeruginosa* PA14 biofilms. Mol Microbiol **51:**675–690. http://dx.doi.org/10.1046/j.1365-2958.2003.03877.x.
33. **Friedman L, Kolter R.** 2004. Two genetic loci produce distinct carbohydrate-rich structural components of the *Pseudomonas aeruginosa* biofilm matrix. J Bacteriol **186:**4457–4465. http://dx.doi.org/10.1128/JB.186.14.4457-4465.2004.
34. **Kuchma SL, Ballok AE, Merritt JH, Hammond JH, Lu W, Rabinowitz JD, O'Toole GA.** 2010. Cyclic-di-GMP-mediated repression of swarming motility by *Pseudomonas aeruginosa*: the *pilY1* gene and its impact on surface-associated behaviors. J Bacteriol **192:**2950–2964. http://dx.doi.org/10.1128/JB.01642-09.
35. **Kuchma SL, Brothers KM, Merritt JH, Liberati NT, Ausubel FM, O'Toole GA.** 2007. BifA, a cyclic-Di-GMP phosphodiesterase, inversely regulates biofilm formation and swarming motility by *Pseudomonas aeruginosa* PA14. J Bacteriol **189:**8165–8178. http://dx.doi.org/10.1128/JB.00586-07.
36. **Nunn D, Lory S.** 1993. Cleavage, methylation, and localization of the *Pseudomonas aeruginosa* export proteins XcpT, -U, -V, -W J Bacteriol **175:**4375–4382.
37. **Kuchma S, Griffin E, O'Toole G.** 2012. Minor pilins of the type IV pilus system participate in the negative regulation of swarming motility. J Bacteriol **194:**5388–5403. http://dx.doi.org/10.1128/JB.00899-12.
38. **Karimova G, Pidoux J, Ullmann A, Ladant D.** 1998. A bacterial two-hybrid system based on a reconstituted signal transduction pathway. Proc Natl Acad Sci U S A **95:**5752–5756. http://dx.doi.org/10.1073/pnas.95.10.5752.
39. **Leake MC, Chandler JH, Wadhams GH, Bai F, Berry RM, Armitage JP.** 2006. Stoichiometry and turnover in single, functioning membrane protein complexes. Nature **443:**355–358. http://dx.doi.org/10.1038/nature05135.
40. **Caiazza NC, Merritt JH, Brothers KM, O'Toole GA.** 2007. Inverse regulation of biofilm formation and swarming motility by *Pseudomonas aeruginosa* PA14. J Bacteriol **189:**3603–3612. http://dx.doi.org/10.1128/JB.01685-06.
41. **Heurlier K, Williams F, Heeb S, Dormond C, Pessi G, Singer D, Camara M, Williams P, Haas D.** 2004. Positive control of swarming, rhamnolipid synthesis, and lipase production by the posttranscriptional RsmA/RsmZ system in *Pseudomonas aeruginosa* PAO1. J Bacteriol **186:**2936–2945. http://dx.doi.org/10.1128/JB.186.10.2936-2945.2004.
42. **Parkins MD, Ceri H, Storey DG.** 2001. *Pseudomonas aeruginosa* GacA, a factor in multihost virulence, is also essential for biofilm formation. Mol Microbiol **40:**1215–1226. http://dx.doi.org/10.1046/j.1365-2958.2001.02469.x.
43. **Ha D-G, Richman ME, O'Toole GA.** 2014. Deletion mutant library for investigation of functional outputs of cyclic diguanylate metabolism in *Pseudomonas aeruginosa* PA14. Appl Environ Microbiol **80:**3384–3393. http://dx.doi.org/10.1128/AEM.00299-14.
44. **Blair DF.** 2003. Flagellar movement driven by proton translocation. FEBS Lett **545:**86–95. http://dx.doi.org/10.1016/S0014-5793(03)00397-1.
45. **Blair DF, Berg HC.** 1990. The MotA protein of *E. coli* is a proton-conducting component of the flagellar motor. Cell **60:**439–449. http://dx.doi.org/10.1016/0092-8674(90)90595-6.
46. **Kojima S, Blair DF.** 2004. The bacterial flagellar motor: structure and function of a complex molecular machine. Int Rev Cytol **233:**93–134. http://dx.doi.org/10.1016/S0074-7696(04)33003-2.
47. **Berg HC.** 2003. The rotary motor of bacterial flagella. Biochemistry **72:**19. http://dx.doi.org/10.1146/annurev.biochem.72.121801.161737.
48. **Minamino T, Imada K, Namba K.** 2008. Molecular motors of the bacterial flagella. Curr Opin Struct Biol **18:**693–701. http://dx.doi.org/10.1016/j.sbi.2008.09.006.
49. **Reid SW, Leake MC, Chandler JH, Lo C-J, Armitage JP, Berry RM.** 2006. The maximum number of torque-generating units in the flagellar motor of *Escherichia coli* is at least 11. Proc Natl Acad Sci U S A **103:**8066–8071. http://dx.doi.org/10.1073/pnas.0509932103.
50. **Tipping MJ, Delalez NJ, Lim R, Berry RM, Armitage JP.** 2013. Load-dependent assembly of the bacterial flagellar motor. mBio **4:**e00551-13. http://dx.doi.org/10.1128/mBio.00551-13.
51. **Morimoto YV, Nakamura S, Kami-ike N, Namba K, Minamino T.** 2010. Charged residues in the cytoplasmic loop of MotA are required for stator assembly into the bacterial flagellar motor. Mol Microbiol **78:**1117–1129. http://dx.doi.org/10.1111/j.1365-2958.2010.07391.x.
52. **Toutain CM, Caizza NC, Zegans ME, O'Toole GA.** 2007. Roles for flagellar stators in biofilm formation by *Pseudomonas aeruginosa*. Res Microbiol **158:**471–477. http://dx.doi.org/10.1016/j.resmic.2007.04.001.
53. **Toutain CM, Zegans ME, O'Toole GA.** 2005. Evidence for two flagellar stators and their role in the motility of *Pseudomonas aeruginosa*. J Bacteriol **187:**771–777. http://dx.doi.org/10.1128/JB.187.2.771-777.2005.
54. **Doyle TB, Hawkins AC, McCarter LL.** 2004. The complex flagellar torque generator of *Pseudomonas aeruginosa*. J Bacteriol **186:**6341–6350. http://dx.doi.org/10.1128/JB.186.19.6341-6350.2004.
55. **Morimoto YV, Nakamura S, Hiraoka KD, Namba K, Minamino T.** 2013. Distinct roles of highly conserved charged residues at the MotA-FliG interface in bacterial flagellar motor rotation. J Bacteriol **195:**474–481. http://dx.doi.org/10.1128/JB.01971-12.
56. **Zhou J, Blair DF.** 1997. Residues of the cytoplasmic domain of MotA essential for torque generation in the bacterial flagellar motor. J Mol Biol **273:**428–439. http://dx.doi.org/10.1006/jmbi.1997.1316.
57. **Zhou J, Lloyd SA, Blair DF.** 1998. Electrostatic interactions between rotor and stator in the bacterial flagellar motor. Proc Natl Acad Sci U S A **95:**6436–6441. http://dx.doi.org/10.1073/pnas.95.11.6436.
58. **Lloyd SA, Blair DF.** 1997. Charged residues of the rotor protein FliG essential for torque generation in the flagellar motor of *Escherichia coli*. J Mol Biol **266:**733–744. http://dx.doi.org/10.1006/jmbi.1996.0836.
59. **Blair DF, Berg HC.** 1988. Restoration of torque in defective flagellar motors. Science **242:**1678–1681. http://dx.doi.org/10.1126/science.2849208.
60. **Paulick A, Koerdt A, Lassak J, Huntley S, Wilms I, Narberhaus F, Thormann KM.** 2009. Two different stator systems drive a single polar flagellum in *Shewanella oneidensis* MR-1. Mol Microbiol **71:**836–850. http://dx.doi.org/10.1111/j.1365-2958.2008.06570.x.
61. **Lele PP, Hosu BG, Berg HC.** 2013. Dynamics of mechanosensing in the bacterial flagellar motor. Proc Natl Acad Sci U S A **110:**11839–11844. http://dx.doi.org/10.1073/pnas.1305885110.
62. **Thormann KM, Paulick A.** 2010. Tuning the flagellar motor. Microbiology **156:**1275–1283. http://dx.doi.org/10.1099/mic.0.029595-0.